

QCD-like technicolor on the lattice

Kari Rummukainen

Department of Physics and Helsinki Institute of Physics, P.O.Box 64, 00014 University of Helsinki, Finland

Abstract. This talk gives an overview, aimed at non-experts, of the recent progress of technicolor models on the lattice. Phenomenologically successful technicolor models require walking coupling; thus, an emphasis is put on the determination of the β -function of various models. As a case study we consider SU(2) gauge field theory with two adjoint representation fermions, so-called minimal walking technicolor theory.

Keywords: technicolor, lattice simulations, conformal window

PACS: 11.15.Ha, 12.60.Nz

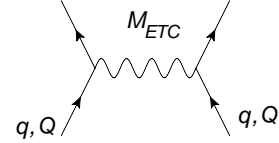
WALKING TECHNICOLOR

The Standard Model, with the Higgs field, is phenomenologically extremely successful. However, the Higgs field has a very special status in the Standard Model (SM): it provides the mechanism for the electroweak symmetry breaking, which is a central feature of the Standard Model. It also is the sole scalar field of the theory, which leads to well-known theoretical problems at energies much higher than the electroweak scale: the hierarchy problem, the stability of the electroweak vacuum, triviality bounds etc. Indeed, many extensions of the SM are motivated by the amelioration of these problems.

In technicolor [1, 2] the symmetry breaking with the fundamental Higgs scalar is substituted with a QCD-like chiral condensate. We remind that QCD already contributes to the electroweak symmetry breaking: the chiral $\bar{q}q$ condensate has electroweak charge, which, if we would remove the Higgs field from the standard model, would alone break the electroweak gauge symmetry and give rise to W and Z boson masses of order f_π (and 3 π -mesons would be absorbed as the longitudinal polarizations of W, Z). In technicolor this mechanism is transferred to the electroweak scale Λ_{EW} . Thus, we introduce a new non-Abelian gauge field, *technigauge*, and massless fermions, *techniquarks* Q . Techniquarks are assumed to have both technicolor and electroweak charge, exactly like quarks in the Standard Model, and they form chiral $\bar{Q}Q$ condensate which breaks the electroweak symmetry. The magnitude of the chiral condensate (or rather, the magnitude of the decay constant f_{TC}) takes the role of the Higgs condensate ($\sim 256\text{GeV}$). Three of the would-be Goldstone bosons, pseudoscalar technimesons, become the longitudinal polarizations of the W and Z bosons. As with QCD, naturally also technicolor has several bound states which would be observable in experiments. This is an elegant and proven mechanism which, in a natural way, describes the electroweak gauge and Higgs sector

without a fundamental scalar particle.

However, the above classic technicolor scenario does not provide for the Standard Model fermion mass terms. This is addressed in the *extended technicolor* theories [3, 4], which produce a Yukawa-like coupling to the technifermion condensate. This can be modeled with a gauge boson with mass M_{ETC} , and which is coupled to the SM fermions (denoted by q) and techniquarks (Q):



At energies smaller than M_{ETC} , this leads to effective four-fermi couplings:

- $g_{ETC}^2/M_{ETC}^2 \bar{Q}Q\bar{q}q$, which gives fermion masses $m_q \propto \langle \bar{Q}Q \rangle / M_{ETC}^2$.
- $g_{ETC}^2/M_{ETC}^2 \bar{q}q\bar{Q}Q$, which contributes to unwanted flavour changing neutral currents.

Precision electroweak measurements strongly constrain flavour changing neutral currents, and this gives the generic constraint $M_{ETC} \gtrsim 1000\Lambda_{EW}$. We recall that the electroweak symmetry breaking pattern requires $\langle \bar{Q}Q \rangle_{TC} \propto \Lambda_{TC}^3 \approx \Lambda_{EW}^3$, where $\langle \rangle_{TC}$ indicates that the condensate is evaluated at the technicolor (\sim electroweak) scale. Naively, the above conditions will give too small SM fermion masses. This can be circumvented if the condensate at the extended technicolor scale is enhanced: we need $\langle \bar{Q}Q \rangle_{ETC} \propto m_q \Lambda_{ETC}^2$.

The renormalization group evolution of the technifermion condensate is

$$\langle \bar{Q}Q \rangle_{ETC} = \langle \bar{Q}Q \rangle_{TC} \exp \left[\int_{\Lambda_{TC}}^{M_{ETC}} \frac{\gamma(g^2)}{\mu} d\mu \right] \quad (1)$$

In a weakly coupled theory the anomalous exponent $\gamma \sim 0$, and the condensate $\langle \bar{Q}Q \rangle$ remains approximately constant. Thus, it is not possible to satisfy the constraints

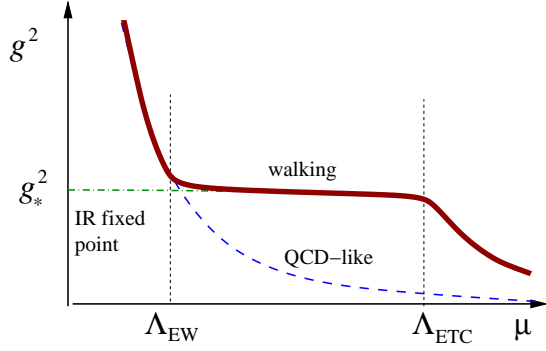


FIGURE 1. The evolution of the walking coupling, versus the QCD-like coupling (dashed line) and the coupling with an infrared fixed point (dash-dotted).

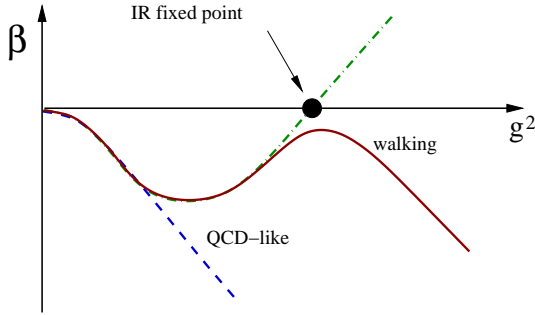


FIGURE 2. The schematic β -functions of theories leading to behaviour shown in Figure 1.

in a QCD-like theory, where the coupling remains large only in a narrow energy range above the chiral symmetry breaking.

However, if the coupling constant *walks* [5, 6, 7], i.e. g^2 remains almost constant $\sim g_*^2$ over the whole energy range from TC to ETC, then

$$\langle \bar{Q}Q \rangle_{\text{ETC}} \approx \left(\frac{\Lambda_{\text{ETC}}}{\Lambda_{\text{TC}}} \right)^{\gamma(g_*^2)} \langle \bar{Q}Q \rangle_{\text{TC}} \quad (2)$$

This is called condensate enhancement. The desired behaviour of the coupling is shown in Figure 1. This makes it possible to satisfy the constraints above, if the anomalous exponent $\gamma(g_*^2)$ is large enough, 1–2.

The β -function

$$\beta = \mu \frac{dg}{d\mu} \quad (3)$$

of the walking theory is shown in Figure 2. The β -function almost reaches zero at some value of the coupling. If the β -function reaches zero at $g^2 = g_*^2$, the theory has an infrared fixed point (IRFP) and the long distance behaviour is conformal, scale invariant. We remind that the value of the coupling at the fixed point is regularisation scheme dependent, but its existence is not. A

theory with an IRFP can be deformed to the walking case by introducing a scale, e.g by adding an arbitrarily small mass term for the techniquarks. Thus, both walking theory or a theory with an IRFP are suitable starting points for a technicolor model.

What kind of theories exhibit walking behaviour? Guidance is given by the 2-loop scheme-invariant β -function of $SU(N)$ gauge theory with N_f fermions of representation R :

$$\beta(g) = -\mu \frac{dg}{d\mu} = -\beta_0 \frac{g^3}{16\pi^2} - \beta_1 \frac{g^5}{(16\pi^2)^2} \quad (4)$$

where $\beta_0 = \frac{11}{3}N - \frac{4}{3}T(R)N_f$, $\beta_1 = \frac{34}{3}N^2 - \frac{20}{3}NT(R)N_f - 4C_2(R)T(R)N_f$, $C_2(R)$ is the second Casimir invariant of the fermion representation R , and $T(R)\delta^{ab} = \text{Tr}T^a T^b$. In asymptotically free theories β_0 must be positive. if $\beta_1 < 0$, the theory is QCD-like; and if $\beta_1 > 0$, then Eq. (4) gives an IRFP at some coupling (Banks-Zaks fixed point [8]). However, generically this fixed point is at strong coupling, and the perturbative analysis is not valid. It is expected that at strong coupling the theory has chiral symmetry breaking, and therefore, the actual *conformal window* where the theory has IRFP is expected to be narrower.

The situation in $SU(N)$ gauge theories with N_f flavours of fundamental, 2-index antisymmetric, 2-index symmetric and adjoint representation fermions is summarized in Figure 3. The conformal windows are shown with shaded regions: the upper edges are where β_0 changes sign, and the lower edges have been estimated with ladder approximation [9]; below this line the system is expected to have chiral symmetry breaking. The lines below the shaded regions show the point where β_2 changes sign. Thus, walking coupling can be expected to be found near the lower edge of the conformal window.

It turns out that the best fit to electroweak precision measurements is obtained using higher than fundamental representations, because in this case the conformal window is reached with a smaller number of fermions [9]. This means that the adjoint representation and 2-index symmetric representation are the most interesting; indeed, the two favourite theories are $SU(2)$ gauge with two adjoint fermions (“minimal walking technicolor”, MWTC), and $SU(3)$ with two 2-index symmetric representation fermions.

THEORIES STUDIED ON THE LATTICE

If a theory is to be a candidate for walking technicolor, it should be in close proximity of the lower edge of the conformal window. It should be either just below the window, in which case it exhibits the walking coupling behaviour, or just within the conformal window. In the lat-

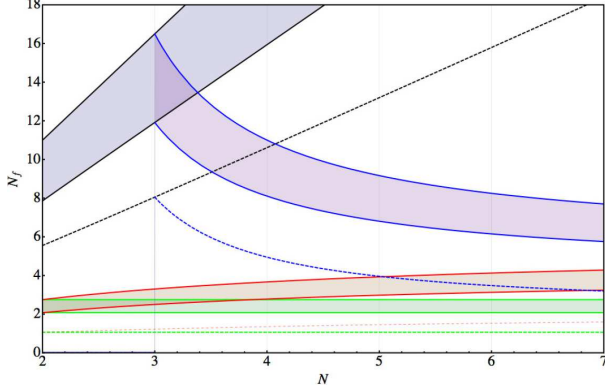


FIGURE 3. The conformal window in $SU(N)$ gauge field theory with N_f fermion flavours in different fermion representations. From top to bottom, the bands correspond to the fundamental, two-index antisymmetric, two-index symmetric and to the adjoint representation fermions. The upper edge of the bands correspond to the loss of the asymptotic freedom, and the lower edge of the band has been calculated using the ladder approximation [9].

ter case the theory is easy to deform into a walking theory by adding a mass or momentum scale to it, e.g. an explicit arbitrarily small mass term for the technifermions. At energy scales less than the mass term the physics is dominated by the gauge fields and the theory confines. Thus, one of the main goals of lattice simulations is to measure the β -function of the theory.

Of the theories shown in Figure 3 the ones with fermions in the fundamental representation are the most familiar, due to their relation with QCD. The most studied case is $SU(3)$ gauge theory with $N_f = 8-16$ flavours of fundamental fermions [10, 11, 12, 13, 14, 15, 16, 17, 18, 19, 20, 21]. These studies indicate that for $N_f \leq 9$ the theory has chiral symmetry breaking and when $N_f \leq 10 \leq 16$ it has an IRFP (however, at $N_f = 12$ results are conflicting, indicating that the systematics with different methods are not yet fully under control). At $N_f > 16$ the theory loses asymptotic freedom.

With $SU(2)$ and fundamental representation fermions the results indicate that for $6 \leq N_f \leq 10$ the theory is within the conformal window [22, 23]. It is not currently known where the lower edge of the conformal window is.

Most interesting theories for technicolor phenomenology are the ones which are at the conformal window with smaller number of flavours. $SU(2)$ with two adjoint representation fermions has been studied by several groups [24, 25, 26, 27, 28, 29, 30]. As described in detail below, there are strong indications that $SU(2)$ with two adjoint fermions is within the conformal window.

There also exist a number of studies of $SU(3)$ gauge with two 2-index symmetric representation fermions [31,

32, 33, 34]. In this case the existence of an infrared fixed point is not fully clarified.

MINIMAL WALKING TECHNICOLOR

Let us have a closer look at $SU(2)$ gauge field theory with two adjoint fermions, “minimal walking technicolor” MWTC, and more precisely, the determination of the β -function, anomalous exponent and the mass spectrum.

β -function in MWTC

Several methods have been used to measure the β -function in the theories discussed here: step scaling with Schrödinger functional scheme [11, 31, 28, 12, 29, 32, 20], Monte Carlo renormalization group [21, 35], Twisted polyakov and twisted Wilson loop schemes [23, 18]. All of these schemes are based on the response of the system when a length scale, typically lattice size, is changed. Here we shall look at the Schrödinger functional method.

In the Schrödinger functional [36] we introduce a constant background field using special boundary conditions and measure the response of the system when the background field is changed. The method was developed and very successfully applied to QCD by the Alpha collaboration [37, 38, 39]. One of the advantages of this method is that simulations with exactly massless fermions are possible: the fixed boundary conditions regulate the eigenvalues of the fermion (Dirac) matrix. Thus, the often cumbersome extrapolation to vanishing fermion masses is avoided.

Consider lattices of volume $V = L^4 = (Na)^4$, where a is the lattice spacing, and following [37], the spatial gauge links on the $x_0 = 0$ and $x_0 = L$ are fixed so that we obtain color diagonal boundary gauge fields

$$A_i(x_0 = 0) = \eta \sigma_3 / (g_0 L) \quad (5)$$

$$A_i(x_0 = L) = (\pi - \eta) \sigma_3 / (g_0 L) \quad (6)$$

Here σ_3 is the third Pauli matrix, and g_0 is the bare gauge coupling. The spatial gauge field boundary conditions are periodic.

At the classical level the boundary conditions above generate a constant Abelian chromoelectric background field, which has an easily calculable action. The derivative of the action with respect to η is $\partial S^{\text{class.}} / \partial \eta = k(N, \eta) g_0^{-2}$, where $k(N, \eta)$ is a known function. By generalizing this to quantum level we obtain the definition for the coupling $g^2(L, a)$:

$$\left\langle \frac{\partial S}{\partial \eta} \right\rangle = \frac{k(N, \eta)}{g^2(L)}. \quad (7)$$

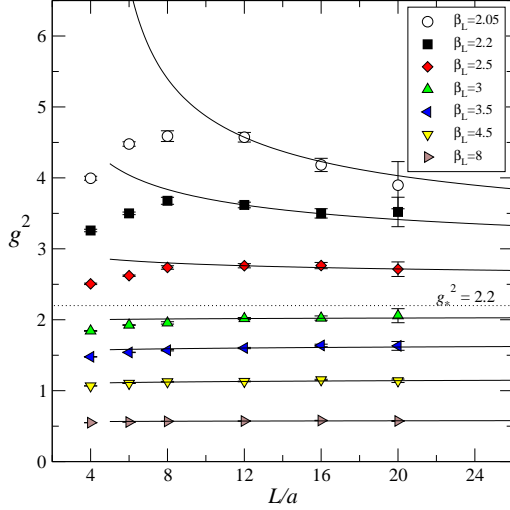


FIGURE 4. The evolution of the measured coupling g^2 in MWTC, SU(2) with 2 adjoint fermions, in the Schrödinger functional scheme. Different plot symbols correspond to different bare couplings $\beta_L \equiv 4/g_0^2$ and hence to different lattice spacings a . Thus, the physical volume between the sets of is very different. The continuous lines show the evolution using a β -function ansatz, Eq. (8) [28].

We fix $\eta = \pi/4$ after taking the derivative. The lhs of Eq. (7) gives a boundary operator which is straightforward to evaluate: in case of unimproved fermions, it is simply the expectation value of the plaquettes touching the boundary. Eq. (7) gives the coupling evaluated at length scale L , the lattice size. Thus, by varying the size of the lattice at fixed lattice spacing a the evolution of the coupling can be measured. By using different lattice spacings a (different lattice gauge couplings g_0) the physical size of the lattice can be changed over a very wide range of length scales.

In a QCD-like theory the β -function is negative, which means that the coupling constant $g^2(L)$ increases as the lattice size is increased while lattice spacing is kept constant. This has been observed in simulations of QCD or SU(2) with two fundamental representation fermions.

In contrast, in MWTC the situation is very different, as shown in Figure 4. What is shown here are measurements of $g^2(L)$ at seven different lattice spacings a and varying lattice size $N = L/a = 4 \dots 20$. Thus, at each lattice spacing we obtain a segment of the evolution when the scale varies over a factor of $20/4 = 5$. Here one observes that when coupling is small (lower sets of data), $g^2(L)$ increases very slowly with increasing lattice size L/a . This is in accord with the two-loop perturbative β -function (4). However, when the coupling increases, the growth slows. Finally, at $g^2 \gtrsim 3$ the measured coupling g^2 decreases with increasing L , if L is large enough, indicating that the β -function is positive. This behaviour is

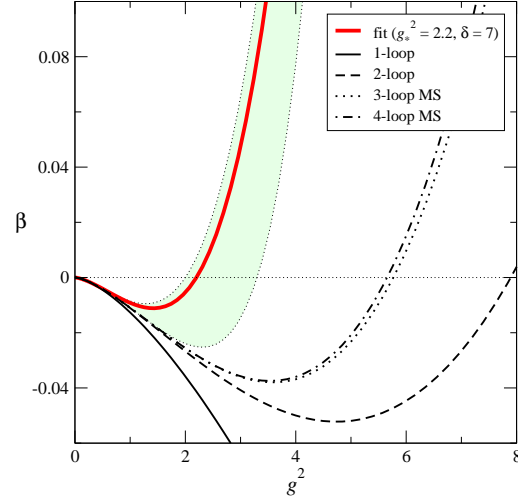


FIGURE 5. The β -function of the MWTC in Schrödinger functional scheme obtained from the fit to the data. The shaded band shows the estimated error range, and the thick line corresponds to fit parameters $g_*^2 = 2.2$, $\delta = 7$. Shown are also the universal 2-loop β -function (dashed line), for comparison, 3- and 4-loop MS-scheme β -functions [40]. Figure from ref. [28].

consistent with an infrared fixed point at $g_*^2 \approx 2-3$. These results are in agreement with the results from [29].

The lattice spacing is a function of the bare lattice gauge coupling $\beta_L \equiv 4/g_0^2$, but a priori we do not its value. The measurements of $g^2(L)$ are used to match the lattices: if, say, we measure a particular value of g^2 on a lattice of size N and coupling g_0 , and the same value of g^2 on a lattice of size $N/2$ and coupling g'_0 , we know that the lattice spacing at g'_0 is twice the one at g_0 .

However, this procedure is made more complicated by finite lattice spacing artifacts. The effect of these can be seen from Figure 4, where at large g^2 the data first increases at small L/a and only starts to decrease at large L/a . The small L behaviour is a finite lattice spacing artifact, and for reliable results a proper continuum limit extrapolation must be used. The standard way to achieve this is to use the step scaling function hierarchially at different lattice sizes (for details, see e.g. [37]). However, because the small volume data is very questionable, this was not attempted here.

The main reason for the difficulty of using the step scaling is that the evolution of $g^2(L)$ in MWTC is very slow, much slower than in QCD. Then the evolution is easily masked by finite lattice artifacts, which are of similar magnitude as in QCD. Improved actions can be expected to help: smaller cutoff effects mean that smaller lattice sizes should become usable in continuum extrapolations.

Nevertheless, one can use the large volume (12^4-20^4) data and check the consistency of the results by fitting a

β -function ansatz:

$$\beta = -L \frac{dg}{dL} = -b_1 g^3 - b_2 g^5 - b_3 g^\delta \quad (8)$$

Here b_1, b_2 are perturbative constants and b_3 and δ are fit parameters, parametrising the location of the fixed point and the slope of the β -function there. Using this fit ansatz the continuous lines in Figure 4 are obtained. The resulting β -function is shown in Figure 5. The error band of the fitted β -function is very large.

For comparison, in Figure 5 also the universal 2-loop β -function is shown. It has the Banks-Zaks fixed point at $g_*^2 \approx 8$, at much stronger coupling than the result from the simulations, $g_*^2 = 2-3$. The Banks-Zaks fixed point is at strong coupling, and perturbative analysis is not reliable. This is indicated by the 3- and 4-loop MS-scheme results also shown in figure [40]; here the fixed point moves substantially towards smaller coupling. It must be emphasized that the MS-scheme values are not directly comparable to the SF-scheme results obtained from the lattice, but are shown to quantify the perturbative uncertainty.

However, the fact that these results are obtained with unimproved Wilson fermion action casts doubts about the validity of the above result: unimproved Wilson action has large $O(a)$ errors, and, as already described above, these make small lattice sizes $L/a < 10$ to be unusable. It would be very welcome to repeat the analysis using fully $O(a)$ improved action. Indeed, large dependence on the action used has been observed in studies of SU(3) gauge with 2-index symmetry representation fermions [32]. Steps toward using non-perturbatively improved action for MWTC have been made in ref. [41].

A large value for the mass anomalous dimension γ around the fixed point is relevant for the condensate enhancement and thus for the success of the extended technicolor model. This can be measured using related Schrödinger functional method. For MWTC this has been done by Bursa *et al.* [29], using the same unimproved Wilson fermion action as was used in the β -function study described above. They observe the anomalous exponent $\gamma(g_*^2)$ to be in the interval 0.09–0.41, too small for the desired walking behaviour. One reason for the small value is that the fixed point is at relatively small coupling, $g_*^2 \approx 2-3$. Because γ is roughly linear function of g^2 , a larger fixed point coupling would correspondingly increase the anomalous exponent.

Particle spectrum in MWTC

In principle, the mass spectrum of the theory should give clear indication of the nature of the theory at long distances: if we assume QCD-like behaviour and chiral

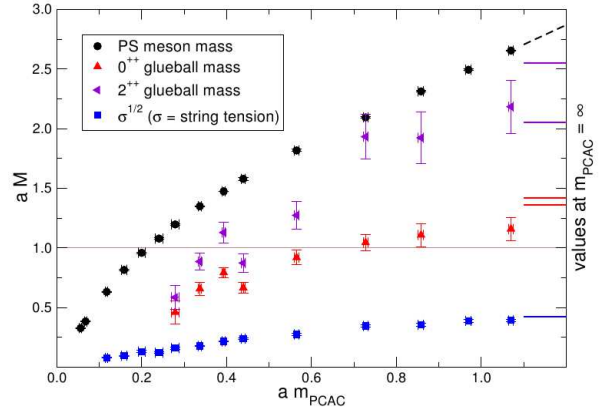


FIGURE 6. The mass spectrum of MWTC as a function of the fermion mass $m_Q a$. All masses vanish as $m_Q \rightarrow 0$. In contrast with QCD, in this case the pseudoscalar is heavier than glueballs or square root of string tension (from [30]).

symmetry breaking, we should observe massless pseudoscalar Goldstone “pions,” whereas other states remain massive as the fermion mass $m_Q \rightarrow 0$.

On the other hand, if the theory has an infrared fixed point, all states become massless as $m_Q \rightarrow 0$, as

$$M \propto m_Q^{1/(1+\gamma(g_*^2))} \quad (9)$$

Thus, this gives another way to measure the mass anomalous exponent.

In Figure 6 the pseudoscalar meson and glueball masses and the string tension are shown against the fermion mass [30]. All states become massless as the fermion mass vanishes, in accordance with the IRFP. In a recent study by Kerrane *et al.* [42] the anomalous exponent $\gamma(g_*^2)$ was measured from the mass spectrum, with the result that it is compatible with zero and certainly $\gamma(g_*^2) \ll 1$.

CONCLUSIONS

Large-scale simulations of theories related with technicolor models started around 3 years ago. During these years the activity has strongly increased and there has been significant progress in methodology. There are now clear indications of the existence of an infrared fixed point in several candidate theories, and the approximate location of the conformal window is also roughly known. Nevertheless, no convincing evidence for a walking coupling has been found yet. However, as the field is still maturing and the computational effort invested in studies grows, we can expect definite results in some candidate theories in the future.

One of the best studied models is the minimal walking technicolor, SU(2) gauge field with two adjoint represen-

tation fermions. There are strong indications about the existence of an IRFP from the β -function and excitation spectrum, at $g_*^2 \approx 2-3$ in SF scheme. In this case the mass anomalous exponent $\gamma(g_*^2)$ appears to be small; too small for the condensate enhancement needed for walking technicolor. This seems to be the case for most candidate models where the anomalous exponent has been studied. However, minimal walking technicolor has been studied only using unimproved Wilson fermions, and in order to have better control of possible lattice artifacts calculations with improved actions are needed.

ACKNOWLEDGMENTS

This work has been supported by the Academy of Finland grant 1134018. The computations described in refs. [28] have been done at the Finnish IT Center for Science (CSC).

REFERENCES

1. S. Weinberg, Phys. Rev. D **19**, 1277 (1979);
2. L. Susskind, Phys. Rev. D **20**, 2619 (1979).
3. E. Eichten and K. D. Lane, Phys. Lett. B **90**, 125 (1980).
4. C. T. Hill and E. H. Simmons, Phys. Rept. **381**, 235 (2003) [Erratum-ibid. **390**, 553 (2004)].
5. B. Holdom, Phys. Rev. D **24**, 1441 (1981).
6. K. Yamawaki, M. Bando and K. i. Matumoto, Phys. Rev. Lett. **56**, 1335 (1986).
7. T. W. Appelquist, D. Karabali and L. C. R. Wijewardhana, Phys. Rev. Lett. **57**, 957 (1986); T. Appelquist, A. Ratnaweera, J. Terning and L. C. R. Wijewardhana, Phys. Rev. D **58**, 105017 (1998).
8. T. Banks and A. Zaks, Nucl. Phys. B **196**, 189 (1982).
9. F. Sannino and K. Tuominen, Phys. Rev. D **71**, 051901 (2005) [arXiv:hep-ph/0405209]; D. D. Dietrich, F. Sannino and K. Tuominen, Phys. Rev. D **72**, 055001 (2005) [arXiv:hep-ph/0505059]; D. D. Dietrich and F. Sannino, Phys. Rev. D **75**, 085018 (2007) [arXiv:hep-ph/0611341].
10. P. H. Damgaard, U. M. Heller, A. Krasnitz and P. Olesen, Phys. Lett. B **400**, 169 (1997) [arXiv:hep-lat/9701008].
11. T. Appelquist, G. T. Fleming and E. T. Neil, Phys. Rev. Lett. **100**, 171607 (2008) [arXiv:0712.0609 [hep-ph]];
12. T. Appelquist, G. T. Fleming and E. T. Neil, Phys. Rev. D **79**, 076010 (2009) [arXiv:0901.3766 [hep-ph]].
13. Z. Fodor, K. Holland, J. Kuti, D. Negradi and C. Schroeder, Phys. Lett. B **681**, 353 (2009) [arXiv:0907.4562 [hep-lat]];
14. Z. Fodor, K. Holland, J. Kuti, D. Negradi and C. Schroeder, Int. J. Mod. Phys. A **25**, 5162 (2010).
15. A. Deuzeman, M. P. Lombardo and E. Pallante, Phys. Lett. B **670**, 41 (2008) [arXiv:0804.2905 [hep-lat]];
16. Phys. Rev. D **82**, 074503 (2010) [arXiv:0904.4662 [hep-ph]];
17. Int. J. Mod. Phys. A **25**, 5175 (2010).
18. E. Itou *et al.*, arXiv:1011.0516 [hep-lat].
19. X. Y. Jin and R. D. Mawhinney, PoS **LATTICE2010**, 055 (2010) [arXiv:1011.1511 [hep-lat]].
20. M. Hayakawa, K. I. Ishikawa, Y. Osaki, S. Takeda, S. Uno and N. Yamada, arXiv:1011.2577 [hep-lat].
21. A. Hasenfratz, Phys. Rev. D **82**, 014506 (2010) [arXiv:1004.1004 [hep-lat]]; Phys. Rev. D **80**, 034505 (2009) [arXiv:0907.0919 [hep-lat]].
22. F. Bursa, L. Del Debbio, L. Keegan, C. Pica and T. Pickup, arXiv:1010.0901 [hep-ph].
23. H. Ohki *et al.*, arXiv:1011.0373 [hep-lat].
24. S. Catterall and F. Sannino, Phys. Rev. D **76**, 034504 (2007) [arXiv:0705.1664 [hep-lat]].
25. A. J. Hietanen, J. Rantaharju, K. Rummukainen and K. Tuominen, JHEP **0905**, 025 (2009) [arXiv:0812.1467 [hep-lat]].
26. L. Del Debbio, A. Patella and C. Pica, arXiv:0805.2058 [hep-lat].
27. S. Catterall, J. Giedt, F. Sannino and J. Schneible, arXiv:0807.0792 [hep-lat].
28. A. J. Hietanen, K. Rummukainen and K. Tuominen, Phys. Rev. D **80**, 094504 (2009) [arXiv:0904.0864 [hep-lat]].
29. F. Bursa, L. Del Debbio, L. Keegan, C. Pica and T. Pickup, Phys. Rev. D **81**, 014505 (2010) [arXiv:0910.4535 [hep-ph]]; F. Bursa, L. Del Debbio, L. Keegan, C. Pica and T. Pickup, arXiv:0910.2562 [hep-ph].
30. L. Del Debbio, B. Lucini, A. Patella, C. Pica and A. Rago, Phys. Rev. D **80**, 074507 (2009) [arXiv:0907.3896 [hep-lat]].
31. Y. Shamir, B. Svetitsky and T. DeGrand, Phys. Rev. D **78**, 031502 (2008) [arXiv:0803.1707 [hep-lat]]; Phys. Rev. D **79**, 034501 (2009) [arXiv:0812.1427 [hep-lat]];
32. T. DeGrand, Y. Shamir and B. Svetitsky, Phys. Rev. D **82**, 054503 (2010) [arXiv:1006.0707 [hep-lat]].
33. Z. Fodor, K. Holland, J. Kuti, D. Negradi and C. Schroeder, JHEP **0911**, 103 (2009) [arXiv:0908.2466 [hep-lat]].
34. J. B. Kogut and D. K. Sinclair, Phys. Rev. D **81**, 114507 (2010) [arXiv:1002.2988 [hep-lat]].
35. S. Catterall, L. Del Debbio, J. Giedt and L. Keegan, arXiv:1010.5909 [hep-ph].
36. M. Luscher, R. Narayanan, P. Weisz and U. Wolff, Nucl. Phys. B **384**, 168 (1992) [arXiv:hep-lat/9207009].
37. M. Luscher, R. Sommer, U. Wolff and P. Weisz, Nucl. Phys. B **389**, 247 (1993) [arXiv:hep-lat/9207010].
38. M. Luscher, R. Sommer, P. Weisz and U. Wolff, Nucl. Phys. B **413**, 481 (1994) [arXiv:hep-lat/9309005].
39. M. Della Morte, R. Frezzotti, J. Heitger, J. Rolf, R. Sommer and U. Wolff [ALPHA Collaboration], Nucl. Phys. B **713**, 378 (2005) [arXiv:hep-lat/0411025].
40. T. van Ritbergen, J. A. M. Vermaseren and S. A. Larin, Phys. Lett. B **400**, 379 (1997) [arXiv:hep-ph/9701390].
41. T. Karavirta, A. M. Mykkanen, J. Rantaharju, K. Rummukainen and K. Tuominen, arXiv:1011.2057 [hep-lat]; arXiv:1011.1781 [hep-lat].
42. E. Kerrane *et al.*, arXiv:1011.0607 [hep-lat].